Pre-Treatment Prediction of Neoadjuvant Chemotherapy Response in Breast Cancer Patients Using DCE-MRI Kinetic Statistics

Ahmed B. Ashraf, Bilwaj Gaonkar, Angela DeMichele, Carolyn Mies, Christos Davatzikos, Mark Rosen, and Despina Kontos

The University of Pennsylvania, Philadelphia, PA 19104, USA,
Ahmed.Ashraf@uphs.upenn.edu

Abstract. The ability to predict response to neoadjuvant chemotherapy for women diagnosed with breast cancer, either before or early on in treatment, is critical to judicious patient selection and tailoring the treatment regimen. In this paper we investigate the role of kinetic features derived from breast DCE-MRI images for predicting treatment response. We present a set of kinetic statistics that differ significantly ($p < 0.05$) between complete responders and non-responders as assessed from imaging exams done prior to the treatment. Based on these features we learn a leave-one-out SVM classifier that performs with AUC=0.91 under the ROC curve. These findings suggest that DCE-MRI kinetic statistics can be used to improve candidate patient selection even before the start of the neoadjuvant treatment.

Keywords: Breast DCE-MRI, kinetic features, classification, neoadjuvant chemotherapy, therapy response prediction

1 Introduction

Use of neoadjuvant chemotherapy in women diagnosed with primary breast cancer is gaining considerable acceptance. It has been reported that neoadjuvant chemotherapy gives high clinical response of up to 70-98%, and can result in a pathologically complete response in 3-34% of patients, [1-4]. On the other hand, it has also been reported that 2-30% of patients may not benefit clinically or pathologically [5]. As a result, the ability to distinguish between highly responsive and non-responsive patients is of critical importance for making treatment choices. Particularly, non-responsive patients, if detected early on, can avoid unnecessary side-effects and can be routed to alternative therapies that may be more effective [5]. Traditionally, therapy response is evaluated by morphological, clinical, and histopathological assessment. Imaging modalities such as computed tomography (CT) and magnetic resonance imaging (MRI) are used to assess tumor response primarily on the basis of tumor size reduction. A notable criterion for therapy response assessment is the Response Evaluation Criterion in Solid Tumors (RECIST) [6]. However, volumetric changes in the tumor due to therapy tend to appear quite late in the course of the treatment. A response as assessed by a reduction in tumor size can cause considerable delay in giving the appropriate treatment to non-responsive patients. As a result devising methods for predicting early therapy response has been an active area of research in recent years.

Among the work on early prediction of therapy response, Ah-See et al. [7] have reported correlations between changes in DCE-MRI kinetic parameters (primarily the rate coefficient, K^{trans}) and the final neoadjuvant chemotherapy response. However, the changes in kinetic parameters in the study presented in [7] had a predictive value after two cycles of neoadjuvant treatment. Moreover, the estimation of K^{trans}, that measures the degree of endothelial permeability, involves a series of assumptions and models derived from the pharmacokinetics of the contrast agent distribution [8]. This leads to different estimates of the parameter due to different underlying assumptions [9], making its estimate less robust. More recently Loo et al. [10] have explored the kinetics and morphology of contrast uptake for predicting a patient's response to neoadjuvant chemotherapy. However, like [7] the approach in [10] also becomes predictive at least after two cycles of chemotherapy treatment which, is also the case for other recent research reports [11]. In this paper, to further investigate the role of imaging as a biomarker for early response in treatment, we address the following two important questions:

(a) Whether imaging biomarkers can help predict therapy response *before* the commencement of the first cycle of neoadjuvant chemotherapy;
(b) Whether DCE-MRI kinetic features derived without modeling assumptions have enough predictive power to predict *a priori* response.

In order to answer the above we explore the kinetic inhomogeneities of the tumor. Specifically we suggest partitioning the tumor pixels into sets based on the similarity of their kinetic behavior (Section 3). We show that within these pixel partitions, the statistics of basic kinetic features (peak enhancement, wash-in-slope, wash-out-slope) differ significantly ($p < 0.05$) between the categories of complete responders and non-responders (Section 5). This analysis is based on breast DCE-MRI images captured *prior* to the treatment. We demonstrate that a support vector machine (SVM) classifier based on these kinetic statistics and using leave-one-out cross validation can predict complete versus non-complete responders with an AUC of 0.91 under the ROC curve (Section 5). These findings suggest that non-model based DCE-MRI kinetic statistics could serve as potential imaging biomarkers for predicting response to neoadjuvant chemotherapy even before the initiation of treatment.

We begin with a brief review of non-model based DCE-MRI kinetic features:

2 DCE-MRI kinetic features

Typically, DCE-MRI acquisition includes a pre-contrast image (captured prior to the injection of a contrast agent) and a number of post contrast images, captured at different time points after the injection of the agent. A usual way to quantify the enhancement pattern is to compute percentage enhancements relative to the pre-contrast image, [12]. By computing the relative enhancement on a pixel by pixel basis we can achieve pixel-wise maps of the contrast enhancement. For a particular pixel, the enhancement plotted as a function of time provides the kinetic curve. As reported in the literature (e.g., [13]), a number of basic features can be computed from this kinetic curve, inlcuding peak enhancement (PE), time to peak (TTP), wash-in-slope (WIS), wash-out-slope (WOS). Figure

1(a) illustrates these features for a single pixel. From these, we can derive a rich kinetic feature set by computing the pixel-wise map for each feature as depicted in Figure 1(b).

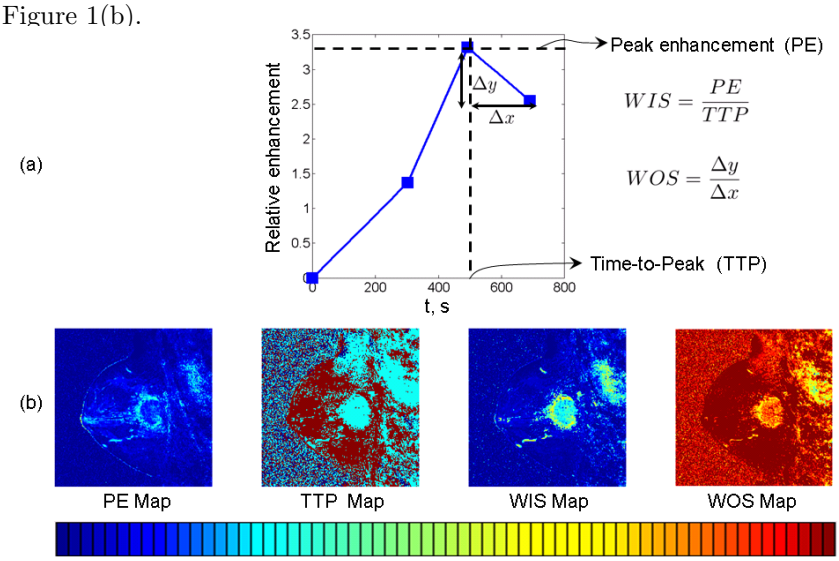

Fig. 1. (a) Illustration of basic kinetic features for a single pixel. (b) Pixel wise maps

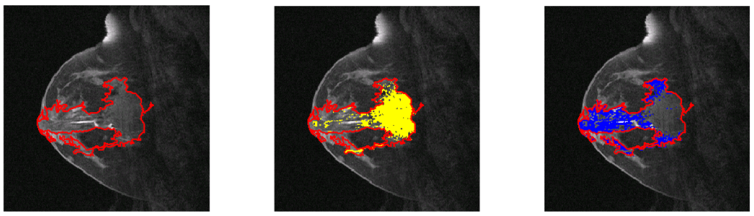

Fig. 2. Illustration of kinetic pixel partitioning for two post contrast time points. (a) Segmented lesion, (b) Set 1 pixels highlighted in yellow, (c) Set 2 pixels highlighted in blue

3 Kinetic partitioning of feature maps

The feature maps shown in Figure 1(b) can be partitioned into different sets based on their kinetic behavior. One way to better interpret the kinetic inhomogeneity is to divide the feature maps into clusters of homogeneity. Here we suggest partitioning the pixels based on their time-to-peak (TTP) value. This step partitions the pixels into as many sets as the number of post-contrast time points. As a result, set i consists of the pixels that achieve their peak enhancement at the i-th post contrast time point. In Figure 2, we illustrate these partitions for two post contrast time points.

3.1 Partition-wise kinetic statistics

Let $\mathcal{M}$ be the pixel partitioning such that $\mathcal{M}_k$ represents the membership mapping of pixel k to its respective set. Based on this partition we may derive the following set-wise statistics:

• Posterior probability of observing Set i given the partition $\mathcal{M}$:

$$\mathcal{P}(\mathcal{S}et = i|\mathcal{M}) = \frac{1}{N}\sum_{k=1}^{N}\delta(\mathcal{M}_k = i)\ . \tag{1}$$

where $\delta(\mathcal{M}_k = i)$ is an indicator function that equals 1 when $\mathcal{M}_k = i$, and zero otherwise. N is the total number of pixels. These N pixels may come from an arbitrarily shaped segmentation mask specifying the lesion.

• Mean value of feature map j for Set i:

$$\mu(i,j) = \frac{\sum_{k=1}^{N} f_j(k).\delta(\mathcal{M}_k = i)}{\sum_{k=1}^{N}\delta(\mathcal{M}_k = i)}\ . \tag{2}$$

where $f_j(k)$ is the value of the j-th feature map for k-th pixel, and the feature map can be any of those shown in Figure 1(b).

• Variance of feature map j for Set i:

$$\sigma^2(i,j) = \frac{\sum_{k=1}^{N}(f_j(k) - \mu(i,j))^2.\delta(\mathcal{M}_k = i)}{\sum_{k=1}^{N}\delta(\mathcal{M}_k = i)}\ . \tag{3}$$

Based on the above definitions, m pixel partitions and n feature maps would result into a total of $m(2n+1)$ features. We aim to investigate the utility of these partition-wise kinetic statistics for the task of predicting response to neoadjuvant therapy.

4 Dataset

The study population consisted of a subset of patients enrolled in a multi-site trial of imaging biomarkers in neoadjuvant breast cancer therapy. The subset population consisted of 15 patients: 8 complete responders and 7 non-responders. All patients presented with biopsy-proven T2-3 stage tumors. The patients underwent standard neoadjuvant chemotherapy, which at the time of the study consisted of four cycles of adriamycin/cytoxan, followed by four cycles of taxotere. Local IRB approval was obtained prior to the study, and signed informed consent was obtained in all patients prior to enrollment. Core biopsy and serum samples were collected at comparable times to the MRI scans and obtained pre-treatment, (between 24 and 96 hours after the start of treatment), between treatment regimens (optional) and pre-surgery. Only pre-treatment imaging was used in the analysis presented in this paper. The treatment response and 3 year disease free survival data were collected.

MRI was performed on a 1.5T scanner (Siemens, Sonata©, Erlangen, Germany). Imaging included sagittal T1-weighted 3D volumetric imaging before and after administration of gadodiamide injection (Omniscan©, GEHealthcare). Imaging parameters were as follows: FOV 18-20 cm, matrix 512×256 (interpolated to 512×512), slice thickness 2mm, TR 27.0, TE 4.76, flip angle 45°. Pre-gadodiamide imaging was performed followed by immediate post-gadolinium images (at 2 minutes) and delayed post-gadodiamide images (at 7 minutes).

For each patient we selected the DCE-MRI exam done prior to the commencement of the treatment. Lesions were segmented in a semi-automated way

by seeding an active contour snake [14]. For feature extraction the most representative slice in an image sequence was chosen as a slice for which the lesion area was maximized. Given a representative slice we computed the kinetic statistics defined in Section 3. For this dataset we had two post-contrast time points and based on the TTP values the pixels were partitioned into two sets ($m = 2$). Within these partitions we computed statistics for three feature maps ($n = 3$) i.e., PE, WIS, and WOS. This resulted in $m(2n + 1) = 14$ kinetic statistics. We also computed the following morphological features: tumor ellipticity [15], tumor circularity [16] (both being measures of shape irregularity), tumor area, and tumor perimeter. In all we had 14 kinetic features and 4 morphological features.

5 Classification experiments

Univariate feature analysis: To analyze the features described above we first performed a t-test analysis using leave-one-out cross validation. For each cross validation fold, we selected the features that differed significantly ($p < 0.05$) between the categories of complete responders and non-responders. In total, 12 out of the 14 kinetic features were selected, which persisted through all leave-one-out cycles. None of the morphological features was selected in any cross-validation fold. Box-plots for the 12 significant kinetic features are given in Figure 3. The ROCs for individual feature classifiers with respective AUCs are given in Figure 4 (AUCs range from 0.78 to 0.86). The univariate classification was based on simple thresholding on individual feature values. This analysis suggests that partition based kinetic statistics potentially possess univariate discriminatory power to distinguish between responders and non-responders from their pre-treatment images.

Multivariate classification: Based on the 12 significant kinetic features selected as a result of the univariate analysis we trained a leave-one-out linear SVM classifier. The SVM classifier was able to distinguish between responders and non-responders with an AUC=0.91 under the ROC curve (Figure 5), improving on the best univariate classifier reported above (AUC: 0.86).

6 Discussion

In this paper we have demonstrated that the statistics derived from the kinetic partitioning of DCE-MRI feature maps (peak enhancement, wash-in-slope, and wash-out-slope) are significant predictors of response to neoadjuvant chemotherapy. We have shown that these statistics have predictive power even when derived from a DCE-MRI exam done prior to the commencement of the treatment. This ability can help in selecting the patients that are expected to benefit the most from the treatment, while routing the anticipated non-responders to alternative therapies without the unnecessary exposure to neoadjuvant treatment. Moreover the kinetic statistics presented here are computed without any modeling assumptions.

Compared to the kinetic features, morphological descriptors demonstrated poor performance. In this paper we have focused on images captured before the treatment begins. As such our results suggest that those morphological features

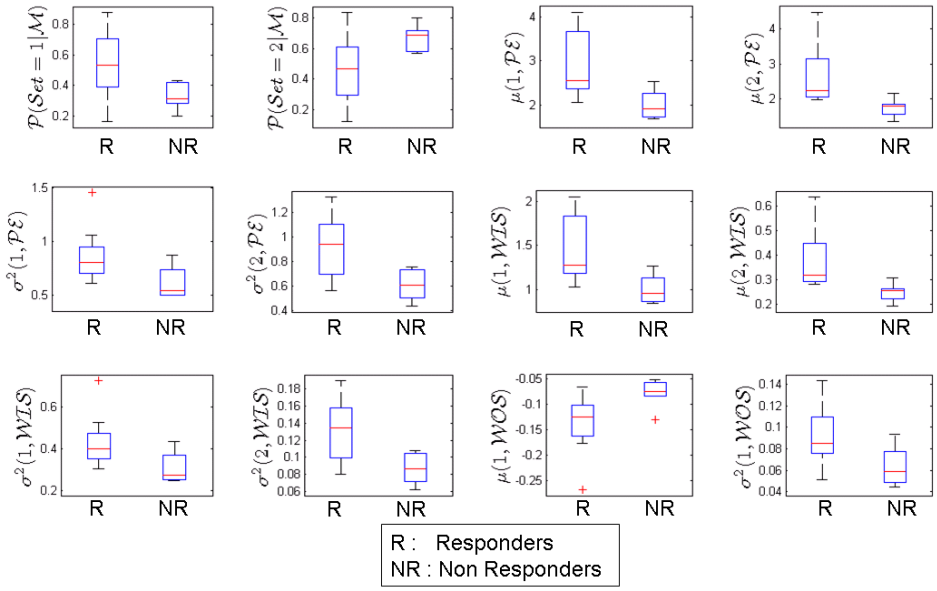

Fig. 3. Box plots for kinetic features that differed significantly (t-test, $p < 0.05$) between the categories. The y-axis shows the respective feature following the notation of Equations 1–3. e.g. $\mu(1, PE)$ represents the mean feature map value of peak-enhancement for Set 1 pixels.

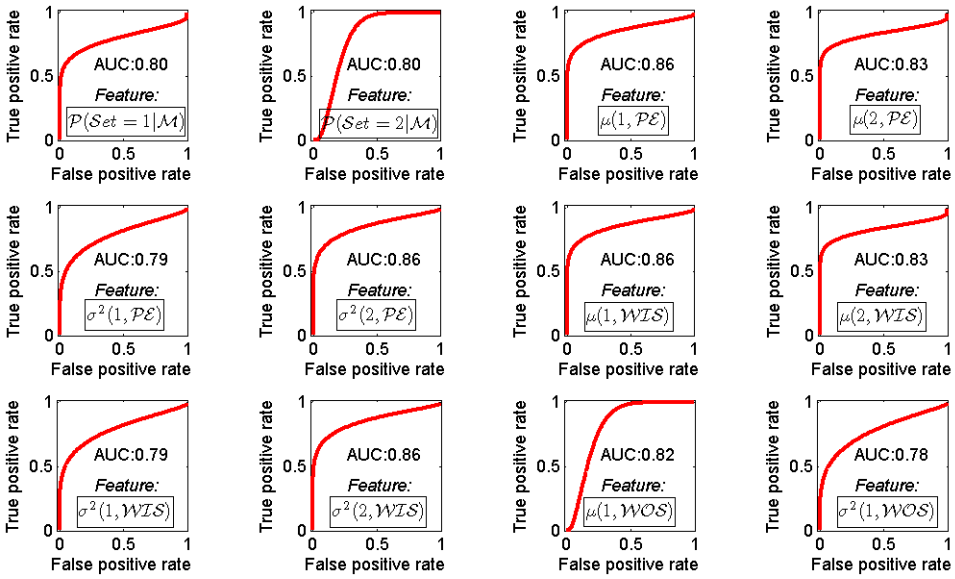

Fig. 4. ROC curves for univariate classifiers.

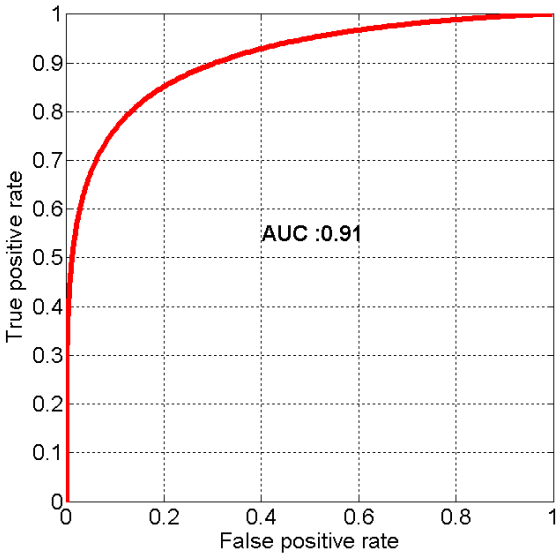

Fig. 5. ROC curves for the multivariate classifier.

fail when presented with the task of predicting therapy response based on a single snapshot of pre-treatment imaging. As the treatment progresses, changes in the morphology during the actual treatment process, rather than the *a priori* imaging on which we focus on this paper, can represent a measure of response as has been explored in other studies.

Two limitations of the current work must be noted. First, although promising, our analysis has been done on a relatively small dataset (15 patients) and therefore larger studies are warranted to confirm generalizability of our findings. Second, the features are currently extracted from a representative 2D slice of the primary lesion. Kinetic partitioning of the entire 3D volume of the lesion could potentially lead to richer statistics that may further improve the prediction of therapy response in the future.

References

[1] Rastogi P., Anderson S.J., Bear H.D., Geyer, C.E., Kahlenberg,M., Robidoux,A., Margolese, R., Hoehn, J., Vogel, V., Dakhil, S., Tamkus, D., King, K., Pajon, E., Wright, M., Robert, J., Paik, S., Mamounas, E., Wolmark, N.: Preoperative chemotherapy updates of National Surgical Adjuvant Breast and Bowel Project Protocols B-18 and B -27, JClin Oncol 26:778-785 (2008)

[2] Bonadonna G.,Valagussa P., Brambilla C., Ferrari, L., Moliterni, A., Terenziani, M., Zambetti, M.: Primary chemotherapy in operable breast cancer: eight-year experience at the Milan Cancer Institute. JClin Oncol, 16:93-100 (1998)

[3] Bear H.D., Anderson S., Brown A., Smith R., Mamounas E., Fisher B., Margolese R., Theoret H., Soran A., Wickerham D., Wolmark N.: The effect on tumor response of adding sequential preoperative docetaxel to preoperative doxorubicin and

cyclophosphamide: preliminary results from National SurgicalAdjuvant Breast and Bowel Project Protocol B-27. JClin Oncol 21:4165-4174 (2003)

[4] Makris A., Powles T.J., Ashley S.E., Chang J., Hickish T., Tidy V.A., Nash A.G., Ford H.T.: A reduction in the requirements for mastectomy in a randomized trial of neoadjuvant chemoendocrine therapy in primary breast cancer. Ann Oncol 9:1179-1184, 1998

[5] Smith I.C., Heys S.D., Hutcheon A.W., Miller I., Payne S., Gilbert F., Ah-See A., Eremin O., Walker L., Sarkar T., Eggleton S., Ogston K.: Neoadjuvant chemotherapy in breast cancer: significantly enhanced response with docetaxel. J Clin Oncol 20:1456-1466, 2002

[6] Hilton, N.: MR imaging for assessment of breast cancer response to neoadjuvant chemotherapy. Magn Reson Imaging Clin N Am.,14(3):383-389 (2006)

[7] Ah-See, M.L.W., Makris,A., Taylor,N.J., Harrison M., Richman P., Burcombe R., Stirling J., dArcy J.A., Collins D.J., Pittam M., Ravichandran D., Padhani A.R.:, Early changes in functional dynamic magnetic resonance imaging predict for pathologic response to neoadjuvant chemotherapy inprimary breast cancer, Clinical Cancer Research, 14(20):65806589, 2008

[8] Cha S., Yang L., Johnson G. Lai A., Chen, M.-H., Tihan T., Wendland M., Dillon W.: Comparison of microvascular permeability measurements,K_{trans}, determined with conventional steady-state T1-weighted and first-pass T2*-weighted MR imaging methods in gliomas and meningiomas. AJNR Am J Neuroradiol. 27:409417, 2006

[9] Tofts P.S., Brix G., Buckly D.L., Evelhoch J.L., Henderson E., Knopp M.V., Larsson H.B., Lee T.Y., Mayr N.A., Parker G.J., Port R., Taylor J., Weisskoff R.M.:. Estimating kinetic parameters from dynamic contrast-enhanced T1-weightedMRIof diffusable tracer: standardized quantities and symbols. J Magn Reson Imaging, 10:223232 (1999)

[10] Loo C.E., Teertstra H.J., Rodenhuis S., van de Viver M.J., Hannemann J., Muller S.H., Peteters M.J., Gilhuijs K.G.: Dynamic contrast-enhanced MRI for prediction of breast cancer response to neoadjuvant chemotherapy: initial results. AJR Am J Roentgenol. 191:13311338 (2008)

[11] Partridge S.C., Vanantwerp R.K., Doot R.K., Chai X., Kurland B.F., Eby P.R., Specht J.M., Dunnwald L.K., Schubert E.K., Lehman C.D., Mankoff D.A.:. Association between serial dynamic contrast-enhanced MRI and dynamic 18F-FDG PET measures in patients undergoing neoadjuvant chemotherapy for locally advanced breast cancer. J Magn Reson Imaging, 32(5):1124-1131 (2010)

[12] Arasu, V. A., Chen, R. C., Newitt, D. N,; Belinda Chang, C., Tso, H., Hylton, N. M., Joe, B. N.: Can Signal Enhancement Ratio (SER) Reduce the Number of Recommended Biopsies without Affecting Cancer Yield in Occult MRI-detected Lesions? Acad Radiol 18:716-721, (2011).

[13] Lee,S.H.,Kim,J.H.,Cho,N.,Park,J.S.,Yang,Z.,Jung,Y.S.,Moon,W.K.,:Multilevel analysis of spatiotemporal association features for differentiation of tumor enhancement patterns in breast DCE-MRI, Med.Phys. 37,3940 (2010)

[14] Kass,M.,Witking,A., Terzopoulos,D.: Snakes: Active Contour Models, IJCV(1988)

[15] Stojmenovic, M., Nayak, A.: Direct Ellipse Fitting and Measuring Based on Shape Boundaries. In: Mery, D., Rueda, L. (eds.) PSIVT 2007. LNCS, 4872:221235 (2007)

[16] Bhooshan,N.,Giger,M.L.,Jansen,S.A.,Li,H.,Newstead,G.M.,: Cancerous breast lesions on DCE MR Images: Computerized characterization for Image based prognostic markers, Radiology, 254(3):680-690 (2010)